SEMI-EMPIRICALLY DERIVED LONG-PERIOD
GROUND MOTIONS GENERATED BY GREAT EARTHQUAKES

D. A. Coats (I)
H. Kanamori (II)
Presenting Author: D. A. Coats

SUMMARY

Long-period ground motions are investigated using a semi-empirical model similar to that advanced by Kanamori (Ref. 1). The model is modified to allow variation in radiation pattern and is applied to a Pt. Conception site. Lower intensity motions of shorter duration are determined for this coastal site compared to those of a Los Angeles site. These differences are interpreted in terms of the geometry and the governing physical model. The model is further extended to three dimensions and applied to a Benioff zone. Successful preliminary hindcasts of the 1968 Tokachi-Oki earthquake indicate the feasibility of the extended model.

INTRODUCTION

Motivation

The purpose of this study is to investigate levels of ground motion generated by a two-dimensional strike-slip simulation model. Additionally, the feasibility of extending the model to a three- dimensional Benioff zone geometry is also explored.

The principal motivation is provided by the need to establish ground motion levels for the design of long-period structures in regions susceptible to great earthquakes ($M_W > 8$). The specification of design ground motions normally requires a set of strong motion accelerograms recorded during earthquakes similar in distance and magnitude to the design event (Ref. 2). An M8+ event is likely to be selected as one of the design events for offshore southern California petroleum platforms since "great" earthquakes have been known to occur along the San Andreas fault in California with recurrence intervals (Ref. 3) similar to those specified by API (Ref. 4). However, no M8+ events have been recorded on strong motion instruments.

In an attempt to circumvent the lack of instrumental data from great earthquakes, Kanamori modeled the 1857 Fort Tejon earthquake which "may be considered a prototype of future great earthquakes on the San Andreas fault system," (Ref. 5). Upcoming OCS lease sales in the southern Bering Sea and the Gulf of Alaska suggest the need for simulation of the much larger Benioff zone earthquakes which occur in the Aleutian islands region.

(I) Senior Research Physicist, Exxon Production Research, Houston, Texas, USA.

(II) Professor of Geophysics, California Institute of Technology, Pasadena, California, USA.

The semi-empirical approach to modeling long-period ground motions is particularly well suited to the development of design criteria for offshore structures. The preferable approach of scaling actual strong motion records is not feasible for great earthquakes since suitable records do not exist (Ref. 2). Smaller earthquakes produce records of a different character and duration than great earthquakes (Ref. 6). Development of design criteria using the semi-empirical simulation approach is, in practice, analogous to the scaling approach. A series of plausible records is simulated by variation in the rupture process and by randomness in the construction of subfault motions. The veracity of these motions is assured by the application of observed seismological constraints. As in the scaling approach, the series of records can be used to develop design spectra with an associated range in levels. Also, individual time-histories can be used for nonlinear structural analysis.

Background

This study is an extension and application of the semi-empirical simulation method advanced by Kanamori (Ref. 1). We will not discuss the details of the model here, but refer the reader to the original paper. However, we will highlight some unique aspects of the simulation approach which make it well suited to the development of design criteria for offshore structures. It has been used in other engineering analyses such as the sloshing induced in large oil tanks (Ref. 7). In this study, the two-dimensional strike-slip model is extended to allow variation in the assumed Love-wave radiation pattern. This modification yields more realistic record simulations which are not as highly transverse polarized. Also, a more complex three-dimensional model is considered for application to a Benioff zone geometry.

In the following sections we will first present a brief description of the theory and mechanics of the simulation method. Next, the results of an application of the strike-slip model to two sites will be compared and discussed. Finally, the feasibility of extending the model to three dimensions will be assessed from a hindcast of the 1968 Tokachi-Oki earthquake using a preliminary model.

MODEL DESCRIPTION

Theory

The original model was designed to generate plausible long-period ground motions emanating from large strike-slip earthquakes which could occur along the southern San Andreas fault in California (Ref. 1). The model convolves an empirical Green's function with a source function describing the space-time history of a multiple shock sequence. As in the previous study, the Green's function is constructed from displacement records observed for the 1968 Borrego Mountain earthquake. A simple amplitude adjustment is made for the effect of geometrical spreading. Thus, the model should not be applied to source/site distances substantially different from those of the Green's function (50-200 km), unless a more universal attenuation relation is included.

An important component of the simulation model is the complexity introduced into ground motion. Rather than an attempt to precisely model the details of rupture propagation, path effects, and subfault dislocation; complexity in ground motions is achieved with a measured amount of randomness in conjunction with the empirically-derived Green's function. As in the original model, the subfault motions are constructed by combining individual Green's functions which are randomly spaced in time.

However, the Love-wave radiation pattern used in the original model may be unrealistic for the heterogeneous earth. Perfect nodes for any of the subfault site geometries are probably not appropriate because of path heterogeneity or non-strike-slip components of faulting. Consequently, we have allowed a 20% variation in the amplitude of the radiation pattern. This amount of variation was used by Hadley and Helmberger (Ref. 8) after a consideration of focal mechanism studies. The random radiation model yields motions that are not as highly transverse polarized, and thus are more representative of actual records.

The simulation approach is particularly well suited to the development of site-specific design criteria for long-period structures such as offshore platforms. In instances, where there is a large disparity between the magnitude of recorded and design events, the scaling approach (Ref. 2) is not feasible, and the synthetic records provide a practical means of estimation. For instance, the empirical basis of the Green's function preserves the stochastic quality of ground motions. Furthermore, variation in the rupture scenario and random number seeds gives some feeling for the range in ground motion levels. From a design standpoint, it is important to consider the variety of possible rupture sequences. The resulting suite of simulated ground motion records can be treated as a set of scaled records in a manner similar to the more empirical approaches (Ref. 2).

Seismological Constraints

The semi-empirical simulation approach is consistent with the philosophy of the design criteria. Simulated ground motion records are not intended to be a precise hindcast or prediction of all the details of motion. What is needed in the development of design criteria are approximate levels of the gross parameters, such as response levels over a broad band, to act as a guide in establishing design spectra. Additionally, an indication of the range in these parameters is needed. This range is a combination of inherent uncertainty due to the stochastic nature of motions (randomness) and variation due to differences in the actual events (rupture propagation).

With respect to this philosophy, the most important aspect of the simulation model is the seismological constraint. Observed seismological constraints, such as the saturation of local magnitude, assures the veracity of the gross parameters derived from the simulation. The simulated ground motions are constrained in three period ranges. The motions at periods close to 1 sec are limited by the observed upper bound on local magnitude. At periods close to 10 sec, the motion is limited by the observed upper bound on the seismic moment of individual subfault shocks. Finally, overall motion levels are constrained to correspond closely to the correct total seismic moment of the entire event. For example, the total seismic moment of the San Andreas design event corresponds to a moment magnitude of M8+.

STRIKE-SLIP APPLICATION

Results

This part of the study was undertaken to investigate ground motions at the Pt. Conception site generated by a great earthquake on the San Andreas fault. Pt. Conception was chosen as a site because of the recent offshore petroleum exploration and production in the region. Simulated ground motions are found to have lower spectral velocities than for a site near Los Angeles. The goal is to characterize the relative levels of long-period motions for different regions. However, these levels should not be used directly in site-specific design since the impact of local faulting and soil properties has not been addressed.

The ground motions are synthesized by dividing the segment of the fault, which broke during the 1857 event, into 17 smaller subsegments. The ground motion resulting from each subsegment is constructed from observed displacement records, which are time-lagged and summed to simulate several different rupture propagations. The geometry of the fault and the Pt. Conception site are sketched in Fig. 1. Three rupture models are considered: (1) FTS model: rupture propagates unilaterally from San Bernardino to Parkfield; (2) FTP model: rupture propagates unilaterally from Parkfield to San Bernardino; (3) FTG model: rupture starts at Fort Tejon (Gorman) and propagates bilaterally.

For each of the three rupture models, three different approaches are used to establish the ground motion generated by the seventeen individual subfaults. The motion from each subfault is obtained by combining actual ground motion records randomly around time lags of 3 and 5 secs. There are three seeds for the random models which generate subfault motions. Combined with the three rupture propagations, nine records are produced for each of the Los Angeles and Pt. Conception sites.

As discussed above, the Love-wave radiation pattern shown in Fig. 1 is too regular to accurately represent the stochastic nature of fault rupture and ground motion propagation. The limited randomness introduced into the radiation pattern serves to model the modification of ground motion resulting from inhomogeneity in the propagating medium or from non-strike-slip components of faulting. It does not affect the overall levels of ground motions when the average of all nine records is considered. However, it is an important consideration when record components from an individual simulation are applied to a structure during a transient time-history analysis.

The average response levels determined for the Los Angeles site (Fig. 2) are consistent with other studies. Again, it is the response level over a broad band that is of interest and not individual response peaks. As expected, response levels for the Los Angeles site are similar to the published values (Ref. 1) despite the added radiation pattern variation. The response levels between 2 and 10 sec are relatively flat and near 50 cm/sec. Design levels recommended by API (Ref. 4) for sites in the region with intermediate soils (Type B) are also close to 50 cm/sec. However, the API design spectrum only extends to 5 sec beyond which this study suggests continuing constant spectral velocity. Note, again, that this study does not consider the impact of ground motions generated by smaller local faults as does API.

The long-period ground motions determined for the coastal site northwest of Los Angeles are lower in intensity than the motions at the Los Angeles site published by Kanamori (Ref. 1). The average response spectra for the two sites indicate that long-period motion levels are approximately 20% lower at the Pt. Conception site (Fig. 2). This is the case even though the average distance to the subfaults is nearly the same for both sites. The difference is mostly a consequence of the nodal position of the coastal site for subfault ruptures along the northern portion of the San Andreas (Fig. 1). The difference between individual components would be greater if the 20% variation in radiation pattern were not included.

There are other differences in the simulated ground motions between the two sites. The differences in the character of displacement time-history are striking for one of the FTS ruptures (Fig. 3). The duration is shorter for the coastal site, and there are two distinct peaks in the envelope of the displacement at the Los Angeles site. These differences in the time-history envelope may result in important differences when progressive nonlinear time domain analyses of structures are performed.

Physical Interpretation

The differences in the ground motions between the Pt. Conception and Los Angeles sites can be interpreted in terms of the governing model. This lends credence to the results obtained for the new coastal site. However, the details of ground motion produced by a particular rupture model should be interpreted cautiously since local geological inhomogeneities are not included and a definitive rupture model cannot be established. On the other hand, the results are adequate for general conclusions concerning the gross parameters such as overall amplitudes and durations.

The less intense response levels obtained at Pt. Conception can be ascribed to the radiation pattern. The model is governed by the Love-wave radiation pattern $\cos 2\phi_i$ where ϕ_i is the azimuth measured from the fault strike of the ith subsegment to a line between the source and the site. Figure 1 shows the geometry and indicates ϕ_i for the Parkfield subsegment. The subsegments along the northern portion of the fault are all in line with the Los Angeles site; i.e., $\phi_i = 0^\circ$. This results in the maximum amplitude in the radiation pattern. On the other hand, ϕ_i for Pt. Conception is generally near 45° for many of the northern subsegments and 135° for southern subsegments. These angles align with nodes in the radiation pattern. Although randomness was included in the radiation pattern, its effect when averaged over the nine different simulations is minimal insofar as overall response levels are concerned.

The shorter duration at Pt. Conception for the FTS Model time-history (Fig. 3) can be ascribed to the Doppler effect of the rupture propagation. The rupture begins near San Bernardino and propagates northward. Thus, the rupture travels toward Pt. Conception for a longer section of fault than it does for Los Angeles. When the rupture propagates toward the site, the ground motion travels in the same direction as the rupture itself and can combine with motions produced by the ongoing rupture, with small time lags. When the rupture is propagating away from the site, the motion produced by ongoing ruptures will fall behind the ground motion which is traveling away from the direction of the ongoing rupture.

The curious double peak in the envelope amplitude of the Los Angeles time-history (Fig. 3) is a consequence of both the radiation pattern and rupture propagation. The initial peak is due to ruptures in the southern portion of the fault which is relatively close to Los Angeles. The second peak arises from the northern portion of the fault where $\phi_i = 0^o$ and amplitude of the radiation pattern is at its maximum. It arrives later because of the time it takes for the rupture to propagate northward, as well as the greater source to site distance.

BENIOFF ZONE APPLICATION

Model

The strike-slip model is extended to a three-dimensional Benioff zone geometry. The rupture takes place on a dipping fault surface. The subducting interface is divided into small two-dimensional subfaults as in the strike-slip case. However, the subfault is assumed to radiate uniformly in all directions since a Love-wave may not dominate the ground motion. As in the strike-slip case, empirical Green's functions constructed of strong motion records from the Borrego Mountain earthquake are combined randomly in time to equal the moment of individual subfaults. In this extension the rupture velocity is assumed to vary randomly with a normal distribution.

Hindcast

The extended model is applied to the geometry of the 1968 Tokachi-Oki earthquake in Japan. Five sites are selected for simulation which correspond to some recording sites at epicentral distances near 200 km (Ref. 9). The same seed values for the random number generator are used in all five simulation cases so the differences reflect the variation due to geometry.

The average response spectra are shown in Fig. 4. The lower solid line is the average of the simulations, and the upper represents the mean-plus-one standard deviation. The dashed line is the average of the observed records and lies near the upper solid line. Thus, the simulated motions are somewhat lower than the observed. However, the range due to variation in site indicates that individual computed and observed spectra overlap.

Discussion

The results of the simulation are encouraging. The three-dimensional model is very preliminary, yet the overall shape and average response level of the simulations match the observed reasonably well. Many parameters of this prototype model are left in their simplest form, and a better match with the observed records could be obtained with more realistic modeling. Some of these parameters include asperity distribution, attenuation, radiation pattern, and a different Green's function. However, the observed records have some unusual features such as impulsive noise at HK003. Consequently, a precise simulation is not justified.

The results do indicate that the extension of the model to the Benioff zone is feasible. Substantial refinement in the details of modeling should lead to defensible ground motion simulations for great subduction-zone earthquakes.

Acknowledgments

This research was supported by Exxon Production Research Company.

REFERENCES

1. Kanamori, H., "Semi-Empirical Approach to Prediction of Long-Period Ground Motion," Bull. Seis. Soc. Am. 69, 1979, pp. 1645-1670.

2. Heaton, T. H., Tajima Fumiko, Mori, A. W., "Estimating Ground Motions Using Recorded Accelerograms, " EERI Seminar reference material: Evaluation of Seismic Hazards, and Decision-Making in Earthquake-Resistant Design. Feb., 1983.

3. Sieh, K. E., "Slip Along the San Andreas Fault Associated with the Great 1857 Earthquake," Bull. Seis. Soc. Am., V. 68, No. 5, Oct., 1978, pp. 1421-1448.

4. "API Recommended Practice for Planning, Designing, and Constructing Fixed Offshore Platforms," American Petroleum Institute, API RP 2A, Thirteenth Edition, 1982.

5. Butler, R., and Kanamori, H., "Long-Period Ground Motion from a Great Earthquake," Bull. Seis. Soc. Am., V. 70, 1980, pp. 943-961.

6. Kanamori, H., and Stewart, G. S., (1978), Seismological Aspects of the Guatemala Earthquake of February 4, 1976, J. Geophys. Res. 83, pp. 3427-3434.

7. Fujino, Y., A.O.H-S. Ang, (1982), Prediction of Seismic Response of Long-Period Structures, Bull. Seis. Soc. Am., V. 68, pp. 1421-1448.

8. Hudley, D. M., and Helmberger, D. V., (1980), Simulation of Strong Ground Motions, Bull. Seis. Soc. Am., V. 70, pp. 617-630.

9. Mori, A. W., and C. B. Crouse, "Strong Motion Data from Japanese Earthquakes," Report SE-29, World Data Center A, Dec., 1981.

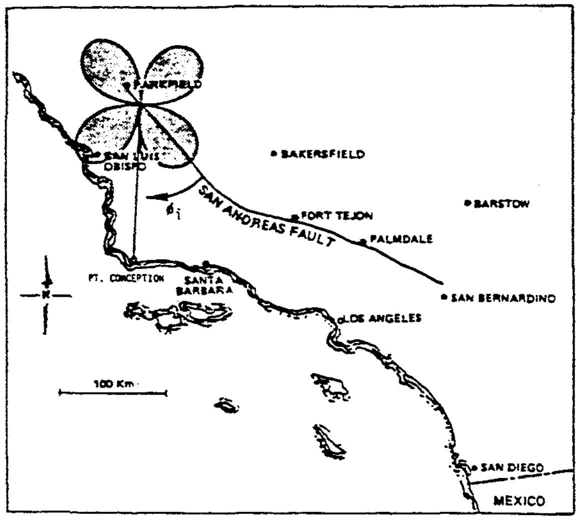

Fig. 1. The segment of the San Andreas Fault used for the computation of ground motions. Also shown is the Love-wave radiation pattern for the Parkfield subsegment.

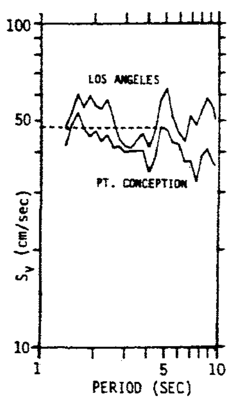

Fig. 2. Average response spectra (5% damping) computed for the Los Angeles and *Pt. Conception sites.* The dashed line is the design level recommended by API for zone 4, soil type B (Ref. 4).

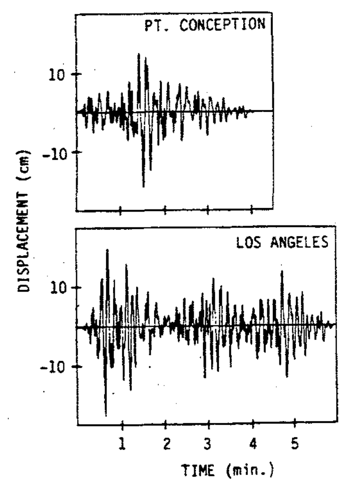

Fig. 3. Displacement time-histories generated by the FTS model at the two sites.

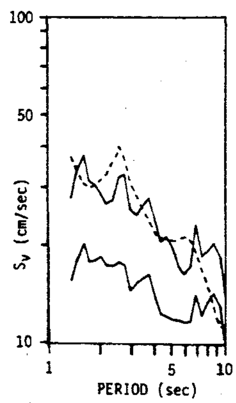

Fig 4. Average response spectra (5% damping) for the Tokachi-Oki earthquake simulation. The solid lines are the average and average plus one standard deviation of the simulated records for five sites. The dashed line is the observed average response for the same five sites: HK003, HK009, TH014, TH020, TH029 (Ref. 9).